calculations at these levels of basis set approximation, there can be cancellation of errors, such that the agreement with observation is not necessarily improved for every type of bond with each improvement of the basis set.[22-24] The discrepancy in the N-H bond lengths is partially accounted for by the lengthening effect of hydrogen bonding, which is calculated to be +0.018 Å in the formamide dimer.[5]

As was observed in the other comparisons of this type, the agreement between the theoretical and experimental valence angles is very good, only exceeding 0.5° for bonds involving hydrogen atoms.

The hydrogen bonding is as described in the X-ray analysis. It consists of hydrogen bond dimers linked laterally to form buckled layers, as in the crystal structure of formamide.[25] The dimensions are shown in Figure 2. There is no hydrogen bonding between layers which have a mean separation of 3.49 Å. It is interesting to note that the lateral hydrogen bonds are slightly shorter and more linear than those involved in the dimer association.

This study provides an example of how high-precision crystal-structure analysis and ab initio theoretical calculations can be used in combination to distinguish between those small distortions which are the intrinsic properties of asymmetrical molecules and those of similar magnitude that arise from crystal-field effects.

Acknowledgment. This research was supported by the National Science Foundation, Grant No. CHE-8117260. Work at Brookhaven National Laboratory was performed under contract with the U.S. Department of Energy. The authors are grateful to Dr. R. K. McMullan for his assistance with the neutron data collection.

Registry No. Thioacetamide, 62-55-5.

Supplementary Material Available: Tables of observed and calculated structure factors for thioacetamide (11 pages). Ordering information is given on any current masthead page.

(22) Binkley, J. S.; Pople, J. A.; Hehre, W. J. *J. Am. Chem. Soc.* **1980**, *102*, 939-947.
(23) DeFrees, D. J.; Levy, B. A.; Pollack, S. K.; Hehre, W. J.; Binkley, J. S.; Pople, J. A. *J. Am. Chem. Soc.* **1979**, *101*, 4085-4089; **1980**, *102*, 2513.
(24) DeFrees, D. J.; Raghavachan, K.; Schlegel, B.; Pople, J. A. *J. Am. Chem. Soc.* **1982**, *104*, 5576-5580.
(25) Ladell, J.; Post, B. *Acta Crystallogr.* **1954**, *7*, 559-564.

Theoretical Comparison between Nucleophilic and Electrophilic Transition Metal Carbenes Using Generalized Molecular Orbital and Configuration Interaction Methods

T. E. Taylor and M. B. Hall*

Contribution from the Department of Chemistry, Texas A&M University, College Station, Texas 77843. *Received July 1, 1983*

Abstract: Ab initio calculations are reported on several transition metal carbenes and their dissociated fragments. In a better than minimal basis set, the orbitals involving the metal-carbene double bond (σ, π, π^*, and σ^*) are optimized by the generalized molecular orbital (GMO) method and used in a full configuration interaction (CI) calculation for the four electrons in the M=C bond. In this manner we maintain the physical significance inherent only in small CI calculations while obtaining the major portion of near-degenerate correlation energy for these four electrons. Our results suggest electrophilic and nucleophilic metal carbenes arise from two different bonding schemes. Electrophilic, 18-electron, metal carbenes can be considered as bonding between singlet metal and singlet carbene fragments, whereas nucleophilic, often electron-deficient, metal carbenes can be considered as bonding between triplet metal and triplet carbene fragments. This conclusion is illustrated using fragment and atomic deformation densities, molecular orbital maps, molecular orbital diagrams, and theoretical thermodynamics. Interchanging singlet and triplet carbene fragments with the metal fragments indicates the metal fragment is slightly more important than the carbene fragment in determining the stability and the electronic properties of metal carbenes. The M=C dissociation energy for electrophilic $(CO)_5Mo{=}CH(OH)$ is calculated to be 60 kcal/mol. The calculated M=C dissociation energy for nucleophilic $CpCl_2Nb{=}CH_2$ is 74 kcal/mol. The latter compound appears to have a stronger π bond. The calculated rotational barrier of the methylene in $CpCl_2Nb{=}CH_2$ is 14.6 kcal/mol, in good agreement with NMR experiments on similar compounds.

Introduction

Transition metal carbene complexes are important to our understanding of many catalytic reactions, including olefin metathesis and Fischer-Tropsch synthesis.[1] Most complexes fall into one of two distinct groups. The Fischer-type complexes,[2] the first of which was $(CO)_5W{=}C(Ph)(OMe)$, are 18-electron species, have the metal in a low (0 or 1+) oxidation state, and are stabilized by heteroatom or phenyl substituents on the carbene carbon. Recently, Schrock prepared a number of tantalum complexes,[3] including $(Me_3CCH_2)_3Ta{=}CH(CMe_3)$ and $(\eta_5\text{-}C_5H_5)_2MeTa{=}CH_2$. These complexes are usually electron deficient (10 to 16 e^-), have the metal in a high oxidation state (3+), and have only hydrogen or simple alkyl substituents on the carbene. Although the M=C bond distance for both types of complexes are similar and in agreement with a typical metal-carbon double bond, there are some important chemical differences. For example, the Fischer-type complexes are electrophilic at the carbon double bonded to the metal, while the tantalum complexes are nucleophilic

(1) (a) Masters, C. *Adv. Organomet. Chem.* **1979**, *17*, 61. (b) Katz, T. J.; Acton, N. *Tetrahedron Lett.* **1976**, *47*, 4251. (c) Schrock, R. R. *Science* **1983**, *219*, 13.
(2) (a) Cotton, F. A.; Lukehart, C. M. *Prog. Inorg. Chem.* **1972**, *16*, 487. (b) Cardin, D. J.; Centinkaya, B.; Doyle, M. J.; Lappert, M. F. *Chem. Soc. Rev.* **1973**, *2*, 99. (c) Fischer, E. O.; Maasböl, A. *Angew. Chem., Int. Ed. Engl.* **1964**, *3*, 580. (d) Fischer, E. O. *Adv. Organomet. Chem.* **1976**, *14*, 1.
(3) (a) Schrock, R. R. *J. Am. Chem. Soc.* **1975**, *97*, 6578. (b) Schrock, R. R. *Acc. Chem. Res.* **1979**, *12*, 98.

0002-7863/84/1506-1576$01.50/0

at this carbon. At first it appears odd that the nucleophilic carbon is associated with the electron-deficient metal. In our view the simplest way to explain these differences involves examination of the metal and carbene fragments.

As we will show, Fischer-type complexes may be viewed as a singlet-state carbene donating to the metal from its "sp^2 hybrid" orbital, with a corresponding amount of back-donation from the metal to the empty π orbital, **1**. Conversely, the tantalum com-

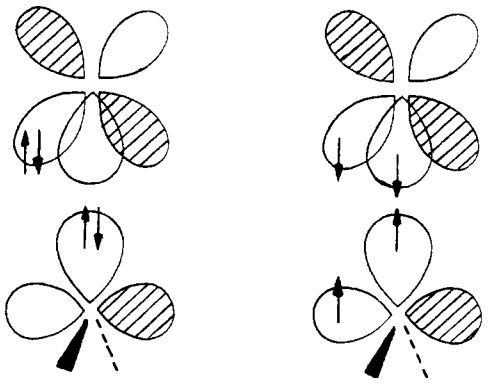

1 2

plexes may be viewed as a triplet-state carbene spin-coupled to two electrons on the tantalum center, **2**. In the Fischer-type complex the π electrons would be polarized toward the metal, while in the tantalum complex the π electrons would be nearly equally distributed. This scheme explains why there is such a dichotomy between these systems. In support of these ideas, calculations on a variety of free carbenes indicate that heteroatom and phenyl substitutions preferentially stabilize the singlet state, while alkyl substitutions stabilize the triplet.[4] One finds phenyls and heteroatom substituents on Fischer-type carbenes and hydrogen and alkyl substituents on Schrock-type carbenes.

Transition metal carbenes have been the subject of several previous theoretical studies. Hoffmann and co-workers have studied metal–hydrogen interaction in the idealized molecule $H_4Ta{=}CH_2$ using extended Hückel calculations.[5] Fenske and co-workers[6] have shown from Fenske–Hall calculations[7] that the site of nucleophilic attack for $(CO)_5Cr{=}C(Me)(OMe)$ is dependent upon the location of the LUMO and have compared the relative π-acceptor abilities of methoxy, amino, and thiomethyl carbenes. Hehre et al.[8] have studied the equilibrium structures and conformational preferences of titanium– and zirconium–methylidene complexes using Hartree–Fock calculations with STO-3G basis sets. Goddard and Rappé have used accurate GVB (generalized valence bond) calculations to study methylene on a bare nickel atom and models for olefin metathesis.[9] Their view of the differences between low- and high-valent metal carbenes is similar to that described in this work. Schaefer et al.[10] have studied the geometry and electronic structure of $(CO)_3Ni{=}CH_2$ at the Hartree–Fock level using an extended basis set. Nakatsuji et al.[11] have studied rotational barriers and the electrophilic character of the Fischer-type complexes, $(CO)_5Cr{=}CH(OH)$ and $(CO)_4Fe{=}CH(OH)$, using minimal basis Hartree–Fock calculations.

In this paper, we report the first accurate calculations of a realistic carbene complex.[12] The calculations use a double-ζ basis set in the region of interest, include significant electron correlation, and have a reasonable ligand environment. Calculations are reported for the five model carbenes, **3–7**.

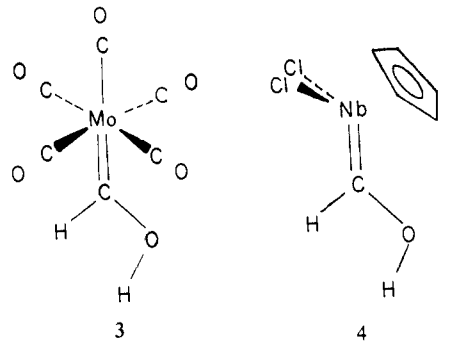

3

4

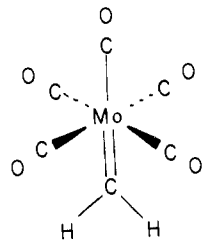

5

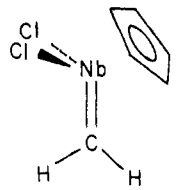

6

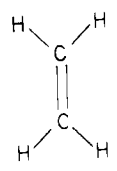

7

Compound 3 is an example of a Fischer-type metal carbene. Although this particular compound has not been isolated, $(CO)_5W{=}C(Me)OMe$ was prepared in 1964 from the nucleophilic addition of lithium methyl to tungsten carbonyl with subsequent acidification and methylation.[13] Fenske–Hall calculations have been performed and demonstrate no major changes in the electronic structure of the metal carbene with the replacement of the methyl groups with hydrogens to give **3**. Compound **6** is representative of electron-deficient tantalum carbenes. This particular carbene has not been isolated; however, $CpCl_2Ta{=}CH(CMe_3)$ was prepared by Schrock by treating $Ta(CH_2CMe_3)_2Cl_3$ with TlCp in toluene.[14] Fenske–Hall calculations demonstrate that replacing the CMe_3 group with hydrogen does not significantly affect the electronic structure. Only one tantalum methylene complex has been made, $Cp_2MeTa{=}CH_2$.[3a]

By interchanging the carbenes of compounds **3** and **6**, one can obtain two more model compounds. Compound **4** has only one synthetic analogue, $(CH_2Ph)Cl(\eta^5\text{-}C_5Me_5)Ta{=}CHPh$.[3b] Compound **5** most closely resembles $(CO)_5W{=}CPh_2$ and $(CO)_5W{=}CHPh$.[15] However, Fenske–Hall calculations imply that the π interactions of the phenyl groups with the α carbon are important for these molecules and cannot naively be replaced with hydrogens. Thus, no synthetic analogue exists for compound **5**. We shall

(4) (a) Baird, N. C.; Taylor, K. F. *J. Am. Chem. Soc.* **1978**, *100*, 1333. (b) Staemmler, V. *Theor. Chim. Acta* **1974**, *35*, 309.
(5) Goddard, R. J.; Hoffmann, R.; Jemmis, E. D. *J. Am. Chem. Soc.* **1980**, *102*, 7667.
(6) (a) Block, T. F.; Fenske, R. F.; Casey, C. P. *J. Am. Chem. Soc.* **1976**, *98*, 441. (b) Block, T. F.; Fenske, R. F. *Ibid.* **1977**, *99*, 4321. (c) Block, T. F.; Fenske, R. F. *J. Organomet. Chem.* **1977**, *139*, 235. (d) Kostic, N. M.; Fenske, R. F. *J. Am. Chem. Soc.* **1981**, *103*, 4677.
(7) Hall, M. B.; Fenske, R. F. *Inorg. Chem.* **1972**, *11*, 768.
(8) Francl, M. M.; Pietro, W. J.; Hout, R. F., Jr.; Hehre, W. J. *Organometallics* **1983**, *2*, 281.
(9) (a) Rappé, A. K.; Goddard, W. A., III *J. Am. Chem. Soc.* **1977**, *99*, 3966. (b) Rappé, A. K.; Goddard, W. A., III *Ibid.* **1982**, *104*, 448.
(10) Spangler, D.; Wendoloski, J. J.; Dupuis, M.; Chen, M. M. L.; Schaefer, H. F., III *J. Am. Chem. Soc.* **1981**, *103*, 3985.
(11) Nakatsuji, H.; Ushio, J.; Han, S.; Yoneyawa, T. *J. Am. Chem. Soc.* **1983**, *105*, 426.

(12) Reference 10 reports accurate calculations on the model compound $(CO)_3Ni{=}CH_2$. However, work reported in this paper implies that this is not a good model for the compounds

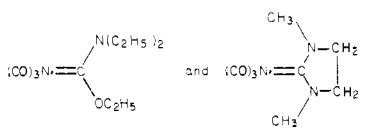

since the model compound has a triplet methylene fragment, rather than the necessary singlet methylene fragment, bonded to the singlet metal fragment.
(13) Fischer, E. O.; Maasböl, A. *Angew Chem.* **1964**, *76*, 645.
(14) (a) McLain, S. J.; Wood, C. D.; Schrock, R. R. *J. Am. Chem. Soc.* **1977**, *99*, 3519. (b) Wood, C. D.; McLain, S. J.; Schrock, R. R. *Ibid.* **1979**, *101*, 3210.
(15) Casey, C. P.; Polichnowski, S. W.; Shusterman, A. J.; Jones, C. R. *J. Am. Chem. Soc.* **1979**, *101*, 7282.

Table I. Molecular Geometries[a]

parameter	3 $(CO)_5Mo{-}CH(OH)$	6 $CpCl_2Nb{-}CH_2$
r MoC-O	1.16[b]	
r Mo-CO	2.02[b]	
r Nb-Cp		2.10[c]
r C_{ring}-C_{ring}		1.42[c]
r C_{ring}-H		1.08[c]
r Nb-Cl		2.35
r metal-C_α	2.14[b]	1.90
r C_α-OH	1.32	
r O-H	0.96	
r C_α-H	1.07	1.07
$\angle$ H-C_α-(OH or H)	108°	108°
$\angle$ C_α-O-H	110°	
$\angle$ Cp-Nb-C_α		112°[d]
$\angle$ Cl-Nb-C_α		103°
$\angle$ Cl-Nb-Cl		103°

[a] Bond lengths are in angstroms. [b] Reference 18. [c] Reference 19. [d] Angles between the centroid of the cyclopentadiene (Cp) ligand and the other three ligands are approximately equal.

compare our results for **3**, **4**, **5**, and **6** with the ample experimental and theoretical data for ethylene, **7**.

Theory

Basis. The basis functions employed in this study were obtained from a least-squares fit of a linear combination of Gaussians to near-Hartree–Fock quality Slater-type functions.[16] The program GEXP processes the functions from the 1s outward, keeping each orbital of higher n quantum number orthogonal to the previous ones. This procedure results in an efficiently nested[17] representation of the function. A contraction of three Gaussian functions represents every basis function occupied in the atomic calculations, except for the metal 3d and 4d orbitals, where four contracted Gaussians are needed to properly fit the original near-Hartree–Fock functions. The most diffuse components of the H 1s, C 2s, C 2p, O 2s, O 2p, Nb 4d, and Mo 4d were split off to form a double-ζ representation. For both metals, the 5s, 5s′, and 5p are represented by single Gaussians of exponents 0.130, 0.043, and 0.124, respectively.

A valence double-ζ basis is employed on the metals and the carbene ligands because the metal–carbene bond is of primary interest in this work, and a high quality basis set of at least double-ζ in that region of the molecule is needed for meaningful results. All atomic orbitals involving core electrons and the other ligands are represented by a minimal basis (fully contracted with three Gaussians per atomic orbital). The four metal carbenes in this study have basis sets ranging from 94 to 105 contracted basis functions.

Geometry. The geometries used in the calculations are summarized in Table I. Although most structure determinations on metal carbenes have involved third-row transition metals, the structures of group 6B hexacarbonyls[20] and $H_3M(C_5H_5)_2$ (where M = Nb, Ta)[19] suggest that the bond distances for both second- and third-row metals will be similar.

An idealized "octahedral" geometry is chosen for the pentacarbonyl molybdenum carbenes. The plane of carbene bisects the carbonyls. The rotational barrier for the carbene is expected to be quite small. The hydrogen on the oxygen is pointed away from the carbonyls. Examples of both this structure[21] and the converse[22] (oxygen substituent pointed toward the carbonyls) exist.

There are a number of crystal structures on 18-electron tantalum carbenes with cyclopentadienyl and chloride ligands where the tantalum chlorine bond distance varies from 2.4 to 2.5 Å.[3b,23] A somewhat smaller metal–chlorine bond distance is expected for our 14-electron species, since there may be a bonding interaction between the chlorine π lone pairs and the electron-deficient metal.

There is also some doubt about the niobium–carbene bond distance in a 14-electron species. An ab initio geometry optimization on the niobium–carbene bond on $Cl_2CpNb{=}CH_2$ indicates that the 14-electron metal–carbene bond distance is similar to known 18-electron tantalum–carbene bond distances, about 1.9 Å. The plane of carbene is perpendicular to the plane of the cyclopentadienyl ring. The hydrogen on the oxygen of hydroxymethylene is pointed away from the cyclopentadienyl because of steric hindrance. Geometries of the methylene and hydroxymethylene ligands are a compromise between singlet and triplet ground states calculated from ab initio studies. The same geometries for the carbene ligands are used for all fragment and all molecular calculations in order to avoid biasing the results. The resultant carbene geometries are in good agreement with crystal structure data on various metal carbenes. The error introduced in dissociation energies by using these fragment geometries at all M=C distances is small.

Generalized Molecular Orbital Theory. The generalized molecular orbital (GMO) approach[24] is a limited type of multiconfiguration self-consistent-field (MCSCF) calculation which provides an optimized set of primary orbitals for configuration interaction (CI) calculations with only modest additional effort beyond that needed for the Hartree–Fock–Roothaan (HF) or standard molecular orbital (MO) approach. In the standard MO approach for a 2n electron closed-shell molecule, the MO's, which have been expanded in a basis set, are divided into a doubly occupied set and an unoccupied set as

$$(\phi_1 \cdots \phi_n)^2(\phi_{n+1} \cdots \phi_m)^0$$

In the GMO approach the previously doubly occupied orbitals are divided into a doubly occupied set and a strongly occupied set, while the previously unoccupied orbitals are divided into a weakly occupied set and an unoccupied set. These four sets of orbitals may be thought of as molecular core, valence, valence correlating, and virtual orbitals, respectively. The electronic configuration in the GMO framework may be written as

$$(\phi_1 \cdots)^2(\cdots \phi_n)^x(\phi_{n+1} \cdots)^y(\cdots \phi_m)^0$$

It is this shell structure, in which the orbitals are treated in groups (sets) with all orbitals in a group (set) having equal occupation numbers, that leads to the use of the name generalized molecular orbital theory.

The GMO wave function consists of a dominant single-determinant, plus a correlation function that contains determinants constructed from all paired excitations from the strongly occupied set to the weakly occupied set. Because all paired double excitations are weighted equally, the energy and wave-function expressions are simplified, and the MO problem can be solved by the Roothaan procedure.[25]

When the variation principle is applied to minimize the energy, the orbitals may be treated in groups as they are in the HF approach. Using a generalized coupling operator[26] to solve this problem, we only need to build two additional HF-like matrices beyond those needed in the ordinary MO approach. Thus, the effort in obtaining optimized orbitals with the GMO procedure is only a small fraction of that needed by a general MCSCF calculation.

(16) Roetti, C.; Clementi, E. *J. Chem. Phys.* **1974**, *60*, 3342.
(17) Marron, M. T.; Handy, N. C.; Parr, R. G.; Silverstone, H. J. *Int. J. Quantum Chem.* **1970**, *4*, 245.
(18) Casey, C. P.; Burkhardt, T. J.; Bunnell, C. A.; Calabrese, J. C. *J. Am. Chem. Soc.* **1977**, *99*, 2127.
(19) Wilson, R. D.; Koetzle, T. F.; Hart, D. W.; Kvick, Å.; Tipton, D. L.; Bau, R. *J. Am. Chem. Soc.* **1977**, *99*, 1775.
(20) Arenesen, S. P.; Seip, H. M. *Acta Chem. Scand.* **1966**, *20*, 2711.
(21) Mills, O. S.; Redhouse, A. D. *Chem. Commun.* **1966**, 814.
(22) Mills, O. S.; Redhouse, A. D. *Angew. Chem.* **1965**, *77*, 1142; *Angew. Chem., Int. Ed. Engl.* **1965**, *4*, 1082; *J. Chem. Soc. A* **1968**, *3*, 642.
(23) (a) McLain, S. J.; Wood, C. D.; Messerle, L. W.; Schrock, R. R. *J. Am. Chem. Soc.* **1978**, *100*, 5962. (b) Churchill, M. R.; Hollander, F. J.; Schrock, R. R. *Ibid.* **1978**, *100*, 647. (c) Daren, J. C.; Prout, K.; DeCian, A.; Green, L. H.; Siganporia, N. *J. Organomet. Chem.* **1977**, *136*, C4.
(24) (a) Hall, M. B. *Chem. Phys. Lett.* **1979**, *61*, 467. (b) Hall, M. B. *Int. J. Quantum Chem.* **1978**, *14*, 613. (c) Hall, M. B. *Int. J. Quantum Chem. Symp.* **1979**, *13*, 195.
(25) Roothaan, C. C. J. *Rev. Mod. Phys.* **1951**, *23*, 69.
(26) (a) Hirao, K. *J. Chem. Phys.* **1974**, *60*, 3215. (b) Hirao, K.; Nakatsuji, H. *J. Chem. Phys.* **1973**, *59*, 1457.

Table II. Optimization of Niobium=Carbene Bond Distance[a]

type of calcn	no. of configurations	bond distance[b]	dissociation energy[c]	force constant[d]
HF	1	1.935	73	4.4
GMO	5	1.958	79	4.1
CI(SD)	9	1.979	72	3.9
CI(SDTQ)	12	1.989	74	3.7[e]

[a] Techniques ordered with increasing electron correlation. [b] Angstroms. [c] Kilocalories mole^{-1}. [d] 10^5 dynes cm^{-1}. [e] Similar to the values of F_2, 4.5, and Cl_2, 3.2.

Details of the computational procedure have been given previously.[24] The choice of orbitals for each of the GMO sets is usually straightforward. A Hartree–Fock–Roothaan calculation is performed on each molecule and the molecular orbitals are assigned. Then, the four orbitals which resemble the σ, π, π^*, and σ^* of the metal–carbon double bond are assigned to the strongly and weakly occupied sets. Application of the GMO procedure localizes both the two strongly occupied orbitals (σ and π) and the two weakly occupied orbitals (π^* and σ^*) into the M=C region. Our previous results on H_2O, N_2, BH_3, and B_2H_6[24c,27] in large Gaussian basis sets showed that the GMO orbitals, both strongly occupied and weakly occupied, resembled the natural orbitals (NO's) of an all singles and doubles excitation CI calculation. The similarity of the orbitals was reflected in the overlap between the GMO's and the NO's, and in the electronic densities and the correlation energies obtained with either set of orbitals.

Configuration Interaction. Following the determination of the GMO's, we have performed configuration interaction calculations within the framework of the four orbitals optimized by the GMO method. The full CI (single, double, triple, and quadruple excitations, SDTQ) has 12 spin-adapted configurations. These 12 configurations account for the major portion of the near-degenerate correlation energy in the metal–carbene double bond.

Valence Bond Orbitals. In a simple system of two molecular orbitals with occupation n_1 and n_2, each electron can be "localized" into valence bond orbitals

$$\phi_{\pm} = \left(\frac{n_1}{n_1 + n_2}\right)^{1/2} \phi_1 \pm \left(\frac{n_2}{n_1 + n_2}\right)^{1/2} \phi_2$$

In a closed-shell Hartree–Fock calculation, n_1 equals 2.0, n_2 equals 0.0; hence $\phi_{\pm} = \phi_1$. However, occupation numbers from calculations including electron correlation range between these two extremes. By taking a linear combination of two orbitals, such as the σ and σ^* orbitals obtained from a full CI calculation, we can obtain localized single electron orbitals similar to those obtained in generalized valence bond calculations.

Computations. All calculations were carried out on Amdahl 470/V6 and V7B computers in double precision at Texas A&M University's Data Processing Center. The integrals and the Hartree–Fock–Roothaan (HF)[25] calculations were done with the ATMOL3 system of programs.[28] The GMO calculations were done with a program written by one of the authors (M.B.H.). The CI calculations were done with a package written by Dr. C. T. Corcoran, Dr. J. M. Norbeck, and Professor P. R. Certain. This package, which was written for a Harris computer, was modified by the authors for the Amdahl 470/V6 and V7B.

Results

Nb=C Bond Distance and Rotational Barrier. Numerous X-ray studies have shown that the tantalum–carbene bond lengths for 18-electron complexes fall in the range of 1.9 to 2.1 Å.[3b,23b,29] Some studies on electron-deficient complexes indicate a smaller bond distance,[30] 1.76 to 1.9 Å, might be more appropriate for complex **6**. An optimization of the niobium–carbene bond length was necessary to eliminate this uncertainty and to provide an accurate dissociation energy. The Nb=C bond distance of **6** was calculated for several types of self-consistent-field calculations. Five points were fit to yield the bond distances shown in Table II. As we improve the calculation by adding electron correlation, the bond distance increases and the force constant decreases. The bond distance for the best calculation, 1.99 Å, is within the range measured in the 18-electron complexes.

Table III. Rotational Barriers in Schrock-Type Metal Carbenes

compound	$\Delta G^{\ddagger}_{rot}$[a]
$Cp_2(CH_3)Ta{=}CHSiMe_3$	17.1
$Cp_2(CH_3)Ta{=}CH_2$	≥21
$Cp_2(CH_2Ph)Ta{=}CHPh$	19.2
$Cp_2(CHPh_2)Ta{=}CHCMe_3$	16.7
$Cp_2ClTa{=}CHCMe_3$	16.8
$Cp_2ClNb{=}CHCMe_3$	15.6
$Cp(PMe_3)_2Ta(=CHCMe_3)_2$	12.5
$CpCl_2Nb{=}CH_2$	14.6[b]

[a] Units in kilocalories per mole. All experimental rotational barriers obtained from temperature-dependent NMR studies (see ref 31). [b] Theoretical determination using techniques described in this paper.

The rotational barrier of the methylene in **6** has also been calculated. The theoretical value of 14.6 kcal mol^{-1} agrees quite well with temperature-dependent NMR determinations of similar compounds shown in Table III. This value represents a lower limit to the π-bond strength, rather than the full strength of the π bond because the π orbital on the carbene can interact with alternative π-type orbitals on the metal as the carbene is rotated.

Wave Functions. The CI coefficients for the five compounds studied are listed in Table IV. The Hartree–Fock ground state is the dominant configuration, and the double excitations are the next most important set of configurations. If the coefficient of the dominant configuration is close to unity, then the Hartree–Fock approximation describes metal–carbene bond accurately. Thus, the Hartree–Fock approximation on the closed-shell ground state describes the metal–carbene bond in the Fischer-type complex, $(CO)_5MoCH(OH)$, better than the bond in the Schrock-type complex, $CpCl_2Nb{=}CH_2$. This is precisely what we would expect if the Fischer-type complex is described best as forming from singlet metal and carbene fragments, and the Schrock-type complex is described best as forming from triplet fragments. The closed-shell Hartree–Fock approximation describes singlet states and electron pair (dative) bonding interactions better than it describes triplet states and unpaired electron (covalent) bonding interactions.

Total Energies. The total energies of the molecules and fragments of interest are listed in Tables V and VI. If a bond in a molecule has a small correlation energy, we might expect it to dissociate into singlet fragments rather than triplet fragments, since correlation effects are generally smaller for singlet interactions[32] (Hartree–Fock works well for interactions involving closed-shell fragments). The data on correlation energies in Table V agree with our contention that compound **3** should dissociate into singlet fragments and compound **6** should dissociate into triplet fragments. The two hybrid molecules, **4** and **5**, appear intermediate in character. The correlation energy of **7** is not completely comparable to **6** because the bonding distances and bonding interactions (p–p vs. d–p) are significantly different.

(27) Taylor, T. E.; Hall, M. B. *J. Am. Chem. Soc.* **1980**, *102*, 6136.
(28) Saunders, V. R.; Guest, M. F. ATMOL 3 System, Atlas Computing Division, Rutherford Laboratory, Chilton, Dedcot, England.
(29) Schrock, R. R., Messerle, L. W.; Wood, C. D.; Guggenberger, L. J. *J. Am. Chem. Soc.* **1978**, *100*, 3793.
(30) (a) Schultz, A. J.; Williams, J. M.; Schrock, R. R.; Rupprecht, G. A.; Fellman, J. D. *J. Am. Chem. Soc.* **1979**, *101*, 1593. (b) Stucky, G. D., unpublished results.
(31) Fellmann, J. D.; Rupprecht, G. A.; Wood, C. D.; Schrock, R. R. *J. Am. Chem. Soc.* **1978**, *100*, 5964.
(32) If a compound dissociates as triplets, the molecular HF wave function does not dissociate properly, and the HF approximation for the molecule is less accurate. Since these calculations are variational, a less accurate approximation means a higher energy and a corresponding larger energy gap between inaccurate (HF) and accurate (CI) calculations.

Table IV. Coefficients of Correlated Wave Functions[a]

configuration	3 $(CO)_5Mo{=}CH(OH)$	4 $CpCl_2Nb{-}CH(OH)$	5 $(CO)_5Mo{=}CH_2$	6 $CpCl_2Nb{=}CH_2$	7 $H_2C{=}CH_2$
Hartree-Fock ground state	0.9828	0.9644	0.9715	0.9614	0.9799
singles					
$\sigma \rightarrow \sigma^*$	0.015	-0.022	0.024	0.012	0.0
$\pi \rightarrow \pi^*$	-0.049	0.042	0.076	-0.011	0.0
doubles					
$\sigma^2 \rightarrow \sigma^{*2}$	-0.074	-0.092	-0.076	-0.094	-0.055
$\pi^2 \rightarrow \pi^{*2}$	-0.110	-0.188	-0.161	-0.194	-0.163
$\sigma^2 \rightarrow \pi^{*2}$	-0.051	-0.027	-0.051	-0.022	-0.013
$\pi^2 \rightarrow \sigma^{*2}$	-0.014	-0.018	-0.014	-0.018	-0.015
$\sigma\pi \rightarrow \sigma^*\pi^*(2)$	0.108	0.164	-0.129	0.163	0.112
	-0.097	-0.107	0.104	-0.104	-0.064
triples					
$\sigma^2\pi \rightarrow \sigma^{*2}\pi^*$	0.008	0.016	-0.010	0.012	0.0
$\sigma\pi^2 \rightarrow \sigma^*\pi^{*2}$	-0.019	-0.014	-0.026	0.004	0.0
quadruples					
$\sigma^2\pi^2 \rightarrow \sigma^{*2}\pi^{*2}$	0.016	0.039	0.024	0.044	0.017

[a] Wave functions obtained from a full CI within the double-bond framework σ, π, π^*, σ^*.

Table V. Total Energy of Molecules[a]

type of calculation	3 $(CO)_5Mo{=}CH(OH)$	4 $CpCl_2Nb{=}CH(OH)$	5 $(CO)_5Mo{=}CH_2$	6 $CpCl_2Nb{=}CH_2$	7 $H_2C{=}CH_2$
Hartree-Fock	-4615.8359	-4938.8408	-4541.8567	-4864.8980	-77.0754
full CI[b]	-4615.8670	-4938.9063	-4541.8990	-4864.9701	-77.1274
correlation energy[c]	-0.0311	-0.0655	-0.0423	-0.0721	-0.0520

[a] Atomic units (hartrees). [b] Twelve configuration full CI. [c] Energy of full CI minus HF energy.

Table VI. Total Energies of Fragments[a]

type of calculation	$(CO)_5Mo$:	$CpCl_2Nb$:	:CH(OH)	$:CH_2$
closed-shell HF	-4503.3688		-112.3877	
singlet[b]	-4503.3726	-4826.3858	-112.3994	-38.4127
triplet[c]	-4503.3066	-4826.4160	-112.3723	-38.4373
ground state	singlet	triplet	singlet	triplet

[a] Atomic units (hartrees). [b] Two configuration GMO calculation. $C_1|\sigma^0\pi^2| + C_2|\sigma^2\pi^0|$. [c] Open-shell Hartree-Fock calculation. $|\sigma^1\pi^1|$.

Dissociation Energies. The orbitals involved in a metal–carbon double bond are σ, π, π^*, and σ^*. During dissociation, each fragment can split off as a triplet, $|\sigma^1\pi^1|$, or as a singlet, $C_1|\sigma^2\pi^0| + C_2|\sigma^0\pi^2|$. By subtracting the ground-state-fragment total energies from the total energy of a full CI calculation (within these four orbitals), we can obtain a reasonable estimate of dissociation energies. Table VII lists the dissociation energies for the five model compounds relative to their ground-state fragments. The dissociation pathways in Table VII are a direct result of the $(CO)_5Mo$: and :CH(OH) fragments preferring the singlet state (by 41 and 17 kcal mol^{-1}, respectively) and $CpCl_2Nb$: and $:CH_2$ fragments preferring the triplet state (by 19 and 15 kcal mol^{-1}, respectively). It is not obvious from this that the dissociation energies of **3**, **6**, and **7**, the compounds having synthetic analogues, should have higher dissociation energies than the hybrid compounds, **4** and **5**, but the results in Table VII show that they do. Apparently, the compatibility of the fragment states plays some role in determining the stability of metal–carbene bonds. Nakatsuji et al.[11] calculated a dissociation energy of 44 kcal mol^{-1} for $(CO)_5Cr{=}CH(OH)$ by subtracting closed-shell fragments from the closed-shell molecule. We calculate a value of 50 kcal mol^{-1} for $(CO)_5Mo{=}CH(OH)$ using the same technique but a better basis set. Electron correlation of both molecule and fragments increases this value to 60 kcal mol^{-1}. Thus, electron correlation is important (10 kcal mol^{-1}) even for $(CO)_5Mo{=}CHOH$, the molecule for which closed-shell HF works best.

An experimental determination of the dissociation energy of ethylene of 163 kcal mol^{-1} [33] is in excellent agreement with our value of 159 kcal mol^{-1}. This implies that our technique, with all its possible errors (small basis set, limited electron correlation, little geometry optimization, ignoring translational, rotational, and zero-point vibrational energies), is reasonably accurate. However, the absolute accuracy of the dissociation energies of the four metal carbene may be in error by as much as 10 to 15 kcal mol^{-1}. In spite of this error, the relative dissociation energies should be reliable. One interesting inference from Table VII is that the molybdenum fragment is less sensitive to the ligand attached to it than the niobium fragment is, since the dissociation energies of **3** and **5** are close than **4** and **6**. It appears that the two molybdenum carbenes have similar dissociation energies because the carbene substituents primarily affect the carbene π system, whereas the Mo=C bond strength is dominated by the σ bond. From a purely thermodynamic point of view, it should be possible to make compound **5**.

Molecular and Valence Bond Orbitals. The molecular orbitals obtained from Hartree–Fock calculations are delocalized and in general cannot be assigned to specific bonds and antibonds. However, generalized molecular orbitals are more localized as are the natural orbitals obtained after the CI calculation.[5] The π, π^*, σ, and σ^* molecular orbitals obtained from a full CI calculation for ethylene are shown in the first and last columns of Figure 1.

An alternative orbital set can be obtained by generating valence bond (VB) orbitals from linear combinations of the previous molecular orbitals. The middle columns of maps of Figure 1 illustrate the VB localized orbitals for each of the four electrons in the π and σ carbon bonds. The two maps in the second column represent two electrons in the carbon–carbon π bond: one electron localized on the top carbon and one electron on the bottom carbon. The electrons in the σ bond are also split between the methylene groups. There are one σ and one π electron on each carbon, consistent with the idea of two methylene triplet fragments bonding to form a double bond (middle column).

Figure 2 shows the single (VB) electron orbitals of the π electrons (left column) and the σ electrons (right column) for our Schrock-type complex, **6**. It is evident that one π electron and one σ electron are localized on each center, in agreement with the scheme of a metal triplet fragment bonding with a methylene triplet fragment (middle column). Figure 3 shows the single electron orbitals for our Fischer-type complex, **3**. Both π electrons are located primarily on the metal, and both σ electrons are located

(33) Benson, S. W. *J. Chem. Educ.* **1965**, *42*, 502.

Table VII. Dissociation Energies of Double Bonds[a]

	3 $(CO)_5Mo{=}CH(OH)$	4 $CpCl_2Nb{=}CH(OH)$	5 $(CO)_5Mo{=}CH_2$	6 $CpClNb{=}CH_2$	7 $H_2C{=}CH_2$
dissociation energy	60	58	56	74	159
metal fragment ground state	singlet	triplet	singlet	triplet	triplet
carbene fragment ground state	singlet	singlet	triplet	triplet	triplet

[a] Units in kcal mol^{-1}.

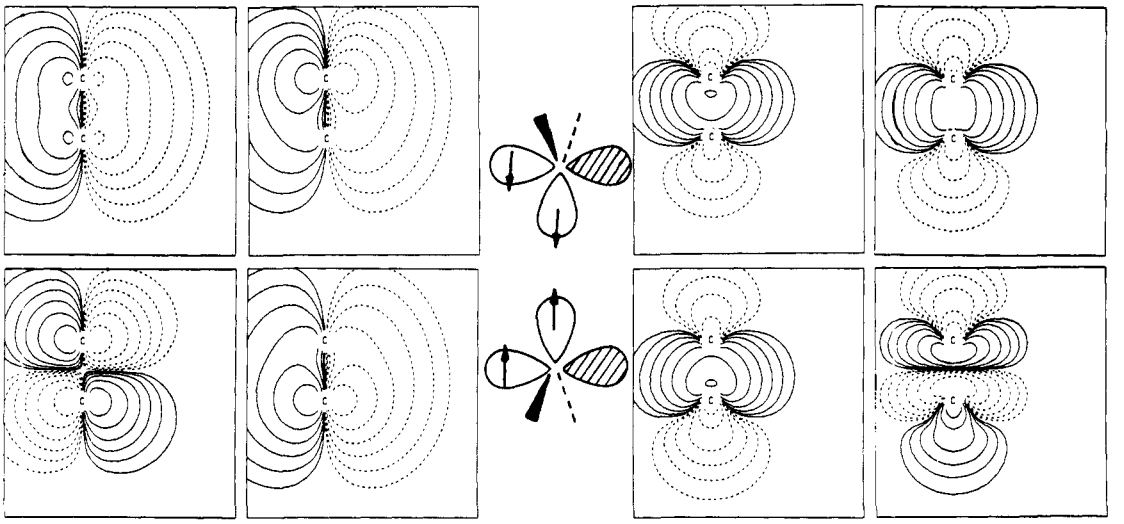

Figure 1. Molecular and VB orbitals of ethylene in the plane of the π bond. The first and last column of maps represent the π, π^*, σ, and σ^* molecular orbitals obtained from our best CI calculation. The second and fourth column represent approximate generalized valence bond orbitals derived from the molecular orbitals; each of these middle four maps represents the localized density of a single electron. The localization of the electrons are shown schematically in the center diagram and show that ethylene can be considered as the bonding of two triplet fragments.

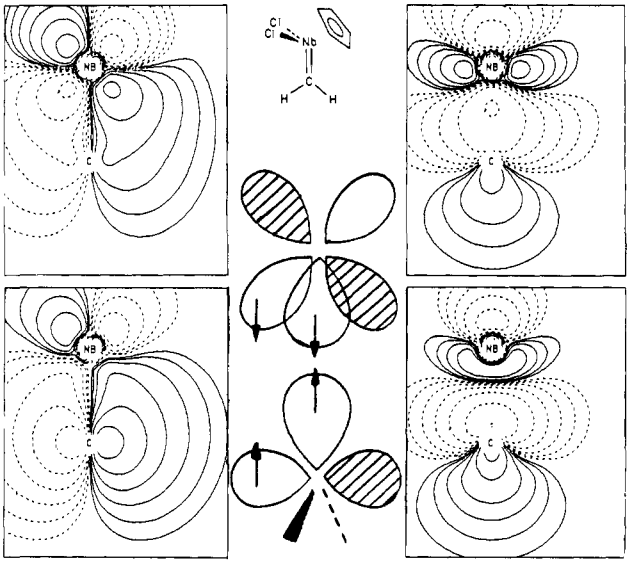

Figure 2. VB orbitals of $CpCl_2Nb{=}CH_2$ in the plane of the π bond. Each map represents the density of one electron. The π electrons and σ electrons are in the left and right columns, respectively. The electrons localize as shown in the center diagram—two triplet fragments.

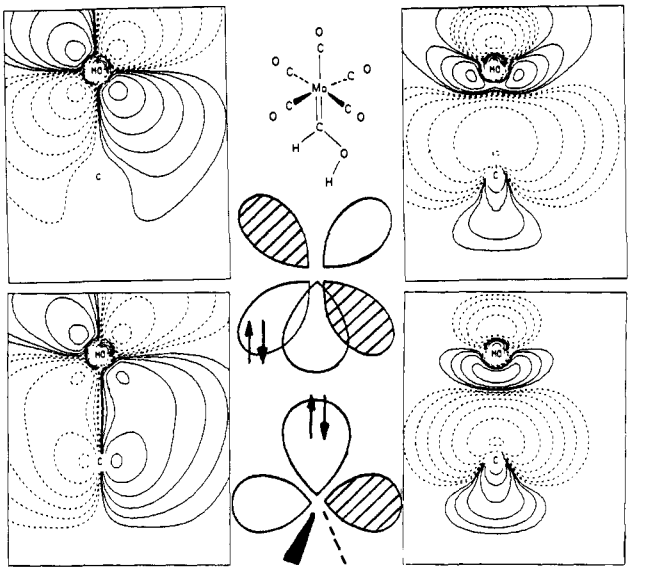

Figure 3. VB orbitals of $(CO)_5Mo{=}CH(OH)$ in the plane of the π bond. Each map represents the electron density of one electron. The π and σ electrons are in the left and right columns, respectively. The electrons localize similarly to that shown in the center diagram—two singlet fragments.

on the carbene. This is consistent with the bonding of a singlet metal fragment, $\sigma^0\pi^2$, with a single carbene fragment, $\sigma^2\pi^0$. Thus the electrons appear to be localized as triplets in ethylene, **7**, and Schrock-type carbenes, **6**, and as singlets in Fischer-type carbenes, **3**.

Compounds **4** and **5** have single electron orbitals intermediate between **3** and **6**. By comparing only the π electron located closest to the carbene carbon for these four compounds (Figure 4), one can separate the effects of the metal and the carbene upon the electron density in double bond. The electron in this VB orbital typifies triplet bonding if localized close to the carbon (compound **6**), and singlet bonding if localized close to the metal (compound **3**). The single π electron of **4** is similar to that of **6**, and that of **3** is similar to that of **5**, implying that the electronic structure of the metal is the major factor in determining the type of bonding present. The other VB electron of this pair is essentially metal based in all molecules.

Electron Densities. By subtracting electron densities of spherical atoms from the electron density of a molecular calculation, one

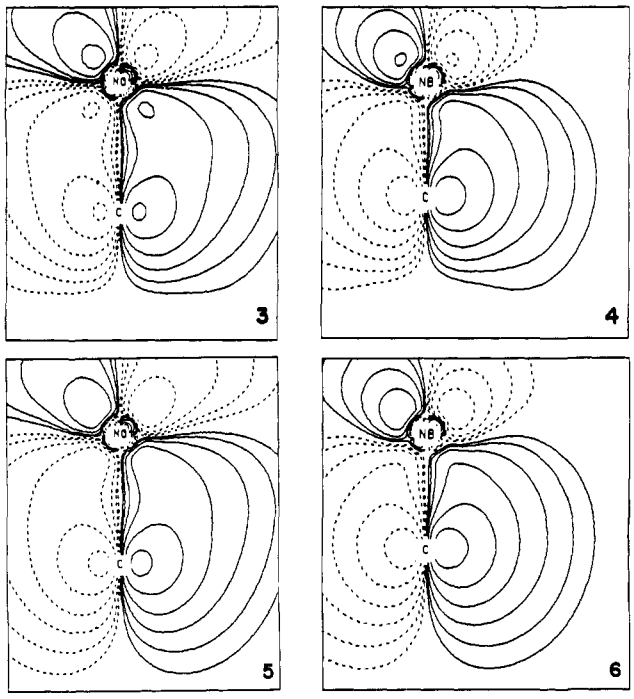

Figure 4. Comparison of a localized electron in the four metal carbenes. The electron illustrated is that of the π electron localized closest to the carbene. The presence of this electron on the carbene implies bonding of triplet fragments (as in **6**) and the presence of the electron on the metal implies bonding of singlet fragments (as in **3**). Compounds **4** and **5** appear intermediate in nature compared with **3** and **6**.

can obtain electron density maps illustrating the deformation of electron densities during molecular formation. Figure 5 illustrates the "atomic deformation" densities for our five model compounds in two planes. Judging from the bonding in the Fischer-type compound, **3** (Figure 3), one might expect extra σ electron density localized on the α carbon carbene and a lack (or decrease) of electron density in the π orbital of the carbene. Indeed, this can be seen in Figure 5. The decrease in the carbene π electron density in part explains the electrophilicity observed in Fischer-type complexes, although other factors are also important.[6] Judging from the last two columns of Figure 5, the carbene fragment in the Schrock-type compound, **6**, is similar to the carbene fragments of ethylene, **7**. The same methylene fragment, bonded to a different metal in **5**, has an obviously different deformation density. It appears that the molybdenum fragment (singlet → triplet energy of 41 kcal mol^{-1}) tends to force the methylene (triplet → singlet energy of 15 kcal mol^{-1}) into the singlet state. This would cause an increase in the methylene σ electron density and a decrease in the methylene π electron density for **5** as compared to **6** and **7**. Using a similar line of reasoning, the substitution of a triplet niobium fragment for the singlet molybdenum fragment in **3** will tend to force the hydroxymethylene into the triplet state. This would cause a decrease in carbene σ electron density and an increase in carbene π electron density in going from compound **3** to compound **4**. All these trends are observed in Figure 5.

Figure 6 shows the fragment deformation densities (molecular minus fragment densities) of compounds **3**, **6**, and **7**. The details regarding these difference densities are somewhat difficult to interpret because the difference densities are strongly dependent on the occupation of the HOMO and LUMO of the fragments. One general statement is reasonable, however. The least rearrangement of electrons occurs when one subtracts those free fragments, which look most like the bound fragments. In looking at compound **3**, we find the lesser rearrangement of electron density to be the top map, molecular minus singlet fragments. In compounds **6** and **7** the lesser rearrangement of electron density occurs in the bottom maps, molecule minus triplet fragments. Thus, the "best" fragments for **3** are singlets and the "best" fragments for compounds **6** and **7** are triplets.

Eigenvalues and Analysis of Molecular Orbitals. Figure 7 illustrates the interaction of two ground-state methylene fragments to form ethylene. The two half-filled σ orbitals in the methylene fragments interact to form a "filled" σ bonding orbital and an "empty" σ^* antibonding orbital; the π orbitals act similarly. As expected, all four molecular orbitals of ethylene can be constructed from equal portions of the methylene fragment orbitals. The molecular orbital diagram for $CpCl_2Nb{=}CH_2$, **6**, is similar to ethylene. Two ground-state fragments interact to form σ and π bonding orbitals and σ^* and π^* antibonding orbitals. An analysis of molecular orbitals of **6** using fragment orbitals shows that each of the four molecular orbitals are constructed from approximately equal portions of fragment orbitals; i.e., no molecular orbital can be definitely associated with a particular fragment. This is quite

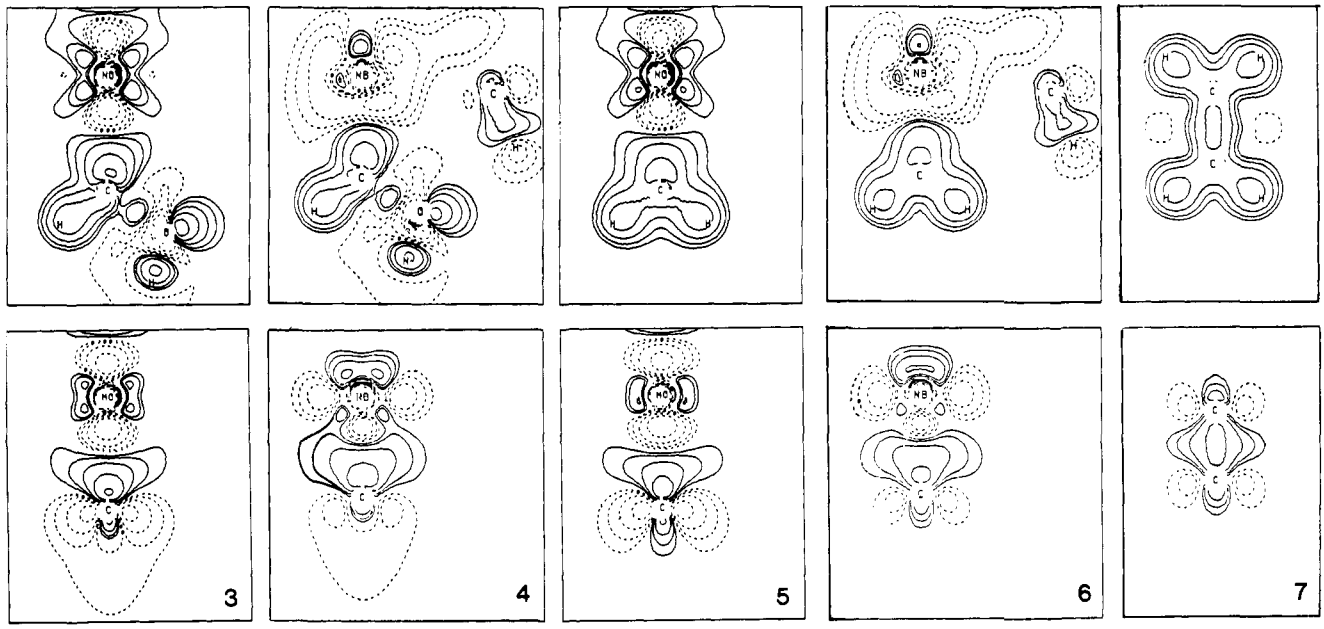

Figure 5. Atomic deformation densities of carbene systems. All deformation density plots in this paper are drawn to the same scale using the same contours. The outer contour represents a change in electron density of $\pm 2^{-7}$ electron (au)$^{-3}$. Each subsequent contour represents an electron density a factor of 2 larger than its neighbor. Atomic deformation densities are calculated by subtracting atomic electron densities from molecular electron densities. They illustrate the redistribution of electrons in going from atoms to molecular systems. The first row and second row of maps represent the atomic deformation densities in the carbene substituent plane and the carbene π plane, respectively.

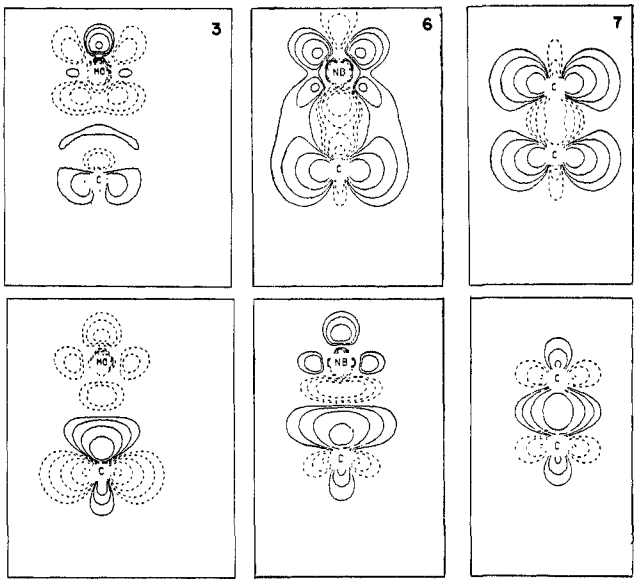

Figure 6. Fragment deformation densities in the plane with the metal–carbene π bond. Fragment deformation densities can be obtained by subtracting singlet (top) or triplet (bottom) fragment electron densities from molecular electron densities. The smallest deformation densities occur when one uses the "best" fragment densities: singlet fragments for compound **3** and triplet fragments for compounds **6** and **7**.

different from the carbene bonding present in $(CO)_5Mo{=}CH(OH)$, **3**. A fragment analysis of **3** indicates each molecular orbital is composed primarily (about 85%) of a particular fragment orbital (Figure 7). The bonding is similar to that of a metal carbonyl; the ligand (carbene) donates in a σ fashion to the metal, and the metal donates to the ligand in a π fashion. Thus, compound **6** seems to bond covalently using triplets, like ethylene, and compound **3** bonds datively using singlets, like a metal carbonyl.

Fragment analyses of molecular orbitals of the hybrid compounds **4** and **5** show that they are of intermediate character. Each molecular orbital in $(CO)_5Mo{=}CH_2$, **5**, is composed primarily (75–80%) of a particular fragment orbital, implying a singlet bonding description is somewhat more appropriate than a triplet bonding description for compound **5**. Each molecular orbital in $CpCl_2Nb{=}CH(OH)$, **4**, is roughly equally shared (about 60%/40%) between the fragments, implying a triplet bonding description is somewhat more appropriate than a singlet bonding description for **4**. For these two compounds, the metal tends to force the carbene into the state the metal prefers for bonding, resulting in double bonds somewhat weaker than the double bonds present in the other two metal carbenes, **3** and **6**.

Extensions to Other Metal–Carbene Systems. Figure 7 shows that :CHOH has a larger σ–π separation than $:CH_2$. The replacement of a hydrogen substituent on a carbene with a heteroatom or phenyl substituent increases the σ–π separation, which in turn stabilizes the low-spin singlet state with respect to the high-spin triplet state.

The major difference between $CpCl_2Nb$: and $(CO)_5Mo$: is the presence of strong π-acceptor ligands on the latter fragment. These ligands stabilize the metal π orbitals, increasing the σ–π separation, which in turn stabilizes the low-spin singlet state. A survey of the chemical literature shows that most metal carbenes fall into one of two classes:

1. Singlet bonding metal carbenes are characterized by strong π-acceptor ligands on the metal, and heteroatom or phenyl substituents on the carbene.

2. Triplet bonding metal carbenes are characterized by the lack of strong π-acceptor ligands on the metal, and hydrogen or alkyl substituents on the carbene.

Metal carbenes that do not fit into one of these two classes generally are characterized by the presence of only one or two π acceptor ligands on the metal, such as $Cp(CO)_2Mn{=}CMe_2$ or $Cp(CO)_2Mn{=}CPh(COPh)$,[34] or by unusual substituents on the carbene such as $CpCl_2Ta{=}CPh(CPh{=}CHCMe_3)$[14b] and $Cp_2W{=}CH(OZrHCp_2)$.[35] The $Cp(CO)_2Mn$ may have a small singlet–triplet separation or may simply have a somewhat weaker M=C bond. Only two compounds are clearly examples of triplet metal bonding to singlet carbene fragments, $(CH_2Ph)Cp_2Ta{=}$

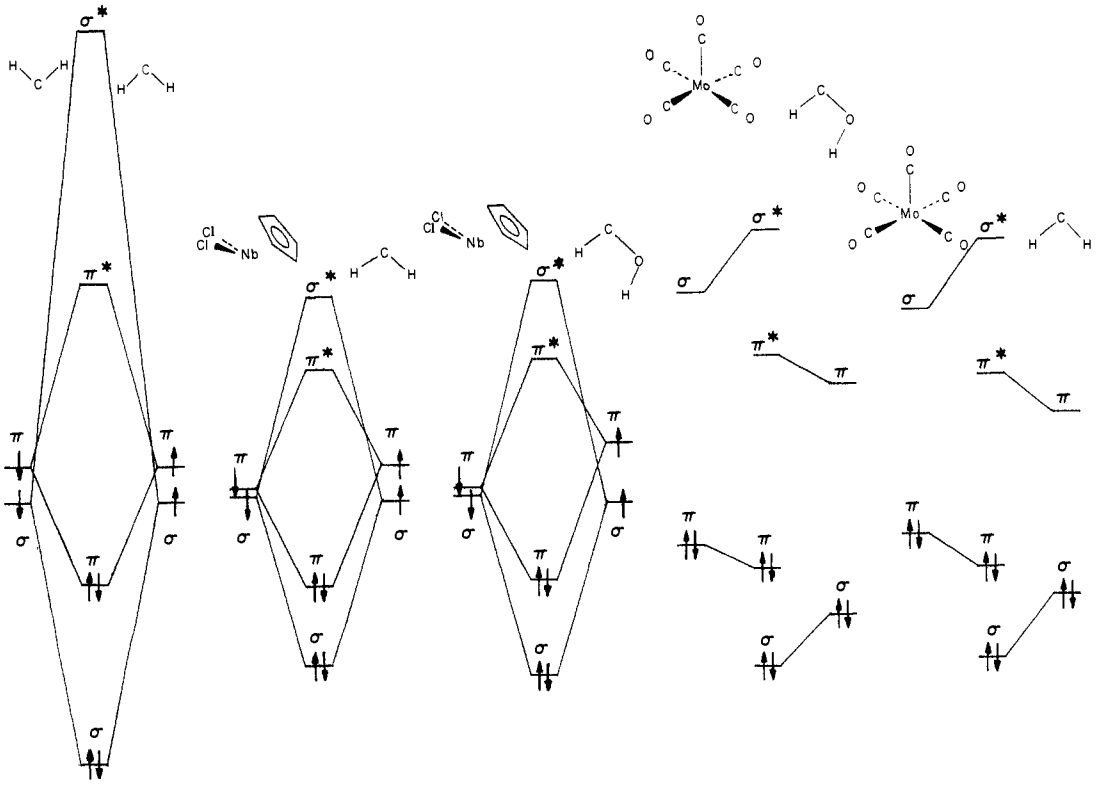

Figure 7. Molecular orbital diagrams of double-bonded systems. Ethylene and $Cl_2CpNb{=}CH_2$ form from triplet ground-state fragments, whereas $(CO)_5Mo{=}CH(OH)$ forms from singlet ground-state fragments. The bonding in the other two molecules is less definite, but $Cl_2CpNb{=}CH(OH)$ is closer to triplet bonding than singlet bonding, and $(CO)_5Mo{=}CH_2$ is closer to singlet bonding than triplet bonding.

$CHPh$[14b] and $(CH_2Ph)Cl(\eta^5\text{-}C_5Me_5)Ta{=}CHPh$.[23a] Our results imply that the metal-carbene bonds of these two compounds are weaker than their alkylidene counterparts. An X-ray crystal structure on $(CH_2Ph)Cp_2Ta{=}CHPh$ supports this idea; the Ta=C bond distance of 2.07 Å is 0.17 Å shorter that a Ta-C single bond, but 0.05 Å longer than a typical Ta=C double bond. A weaker than normal Ta=C bond would make these two compounds interesting candidates for catalytic studies.

Conclusion

Through the use of a properly designed basis set (doubleζ in the metal carbene, minimal basis elsewhere) and limited electron correlation (GMO and CI methods) within the double bond, reasonable electron densities and dissociation energies can be calculated on large metal-carbene systems.

A calculation on ethylene using the same techniques and basis set yields a bond dissociation energy only 4 kcal mol^{-1} less than the experimental estimate of 163 kcal mol^{-1}. A partial geometry optimization on $CpCl_2Nb{=}CH_2$ indicates this electron-deficient complex has a Nb=C bond distance, 1.99 Å, similar to well-characterized 18-electron complexes. The calculated rotational barrier of the methylene in $CpCl_2Nb{=}CH_2$ is 14.6 kcal mol^{-1}, in good agreement with experimental determinations of similar compounds. This value also sets a lower limit on the π bond energy of $CpCl_2Nb{=}CH_2$, since the π bond is only partially broken when the methylene group is rotated 90°. The other three metal carbenes studied have bond dissociation energies 14 to 18 kcal mol^{-1} less than $CpCl_2Nb{=}CH_2$, apparently because of weaker π bonds in these complexes.

Several independent techniques (dissociation energies, single electron valence bond density plots, atomic deformation densities, fragment deformation densities, molecular orbital diagrams, and fragment analysis of molecular orbitals) illustrate the electronic difference between Fischer-type metal carbenes and Schrock-type tantalum carbenes. The former bind datively as singlet fragments, whereas the latter bind covalently as triplet fragments.

Acknowledgment. This work was supported by the National Science Foundation (CHE79-20993 and CHE83-09936) and the National Resource for Computation in Chemistry (National Science Foundation Grant No. CHE77-21305). The authors thank Professor R. Schrock for the opportunity to present this work in the Symposium on the Chemistry of Unsaturated Metal-Carbon Bonds at the 184th American Chemical Society Meeting, Kansas City, Sept. 12-17, 1982.

Registry No. 3, 88589-51-9; **4**, 88609-69-2; **5**, 88589-52-0; **6**, 88589-53-1; **7**, 74-85-1.

(34) (a) Friedrich, P.; Besl, G.; Fischer, E. O.; Huttner, G. *J. Organomet. Chem.* **1977**, *139*, C68. (b) Redhouse, A. D. *Ibid.* **1975**, *99*, C29. Similar Fe compounds are also known; see Brookhart, M.; Tucker, J. R.; Husk, G. R. *J. Am. Chem. Soc.* **1981**, *103*, 979. Brookhart, M.; Tucker, J. R.; Flood, T. C.; Jensen, J. *Ibid.* **1980**, *102*, 7802.

(35) Wolczanski, P. T.; Threlkel, R. S.; Bercaw, J. E. *J. Am. Chem. Soc.* **1979**, *101*, 218.

Calculation of Electron Tunneling Matrix Elements in Rigid Systems: Mixed-Valence Dithiaspirocyclobutane Molecules

David N. Beratan* and J. J. Hopfield†

Contribution No. 6850 from the Division of Chemistry and Chemical Engineering, California Institute of Technology, Pasadena, California 91125. *Received August 4, 1983*

Abstract: A semiempirical model is presented which predicts photoassisted electron-transfer rate dependence on distance for redox groups connected by rigid polymeric linkers. The model approximately reproduces the observed decay of the optical tunneling matrix element with distance found for the rigid ruthenium dithiaspiro mixed-valence complexes of Stein, Lewis, Seitz, and Taube.[1-3] The method calculates the through-bond propagation of the wave function tail, by a method which emphasizes obtaining the correct distance dependence of the tunneling matrix element for these weakly interacting donor-acceptor complexes. The method also allows prediction of the magnitude of the matrix element, the importance of hole or electron tunneling in the transport process, the effect of donor and acceptor redox potential on the matrix element, and the thermal tunneling matrix element for these and other compounds.

Introduction

Electron-transfer theory predicts an approximately exponential decrease in electron-transfer rate with distance when the donor and acceptor weakly interact.[4-6] Only recently, however, have rigid molecules with weakly interacting electron donor and acceptor groups become available.[1-3,7,8] Predictions of transfer rates, qualitative in the past, must be refined to treat this new class of compounds. A series of mixed-valence ruthenium molecules (I, II, III) was recently synthesized and studied by Stein, Lewis, Seitz, and Taube.[2,3]

Interaction between the metal ions is believed to be rather weak and to involve through-bond rather than through-space interactions.[2,3,9] If the interaction between donor and acceptor is indeed weak, one may imagine that relaxation of vibrational modes in the molecule and of the solvent around the odd electron (vibronic coupling) stabilizes the localization. This relaxation provides a deeper well for the electron on one side of the molecule compared to the otherwise equivalent site. Hence one finds, for a short time at least, a ground state for the odd electron localized on one relaxed

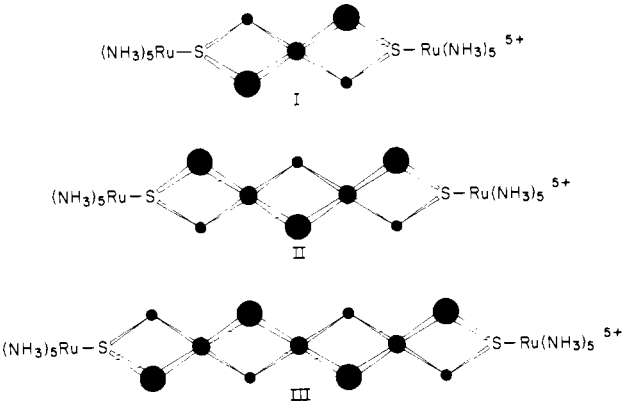

† Also California Institute of Technology, Division of Biology, and Bell Laboratories, Murray Hill, NJ 07974.

(1) Taube, H. In "Tunneling in Biological Systems"; Chance, B., DeVault, D. C., Frauenfelder, H., Marcus, R. A., Schreiffer, J. R., Sutin, N., Eds.; Academic Press: New York, 1979, pp 173-199.

(2) Stein, C. A.; Taube, H. *J. Am. Chem. Soc.* **1981**, *103*, 693-695.

(3) Stein, C. A.; Lewis, N. A.; Seitz, G. *J. Am. Chem. Soc.* **1982**, *104*, 2596-2599.

0002-7863/84/1506-1584$01.50/0